J. COMBIN. MATH. COMBIN. COMPUT. 127b (2025) 779--793

Journal of Combinatorial Mathematics
and Combinatorial Computing
www.combinatorialpress.com/jcmcc

Combinatorial Press

Implications of Finite Element Method-based Analysis of Wushu Movement Mechanics for Performance Techniques and Injury Prevention

Yayun Ji[1, ✉]

[1] *School of Physical Education, Huanghuai University, Zhumadian, Henan, 463000, China*

ABSTRACT

In this paper, the 3D reconstruction of the finite element model of the knee joint is completed by first generating and editing the 3D images of the martial arts movements through Mimics software. After that, Hypermesh and Abaqus software are used to pre- and post-process the properties of materials in the knee joint biomechanical finite element model. Visual 3D software and low-pass filter smoothing technique were used to obtain and process the kinematic and kinetic data of the martial arts maneuvers, and the processed data were used as boundary and loading conditions to import the data of the three martial arts maneuvers, namely, horse stance, lunge stance, and servant stance into the finite element model for calculating and comparing the biomechanical responses of the articular cartilage and meniscus. The results showed that the movement pattern of horse stance has a larger knee range of motion and a smaller peak ground reaction force compared to the lunge and servant stance movements in the martial arts maneuvers. Finite element simulations showed that the straddling knee stance produced smaller peak contact stresses on the knee cartilage and meniscus, and the peak stress area changed more during the movement. Three-dimensional finite element simulation analysis obtained four characteristic moments, namely: the first peak ground reaction force moment, the maximum external rotation-external rotation moment, the maximum dorsiflexion moment, and the second peak ground reaction force moment, which corresponded to a greater difference in ground reaction force values. Therefore, it is recommended to wear protective equipment in advance for the injury-prone areas to reduce the risk of injury before the wushu performance.

Keywords: Wushu movements, knee joint finite element model, ligament mechanical properties, low-pass filter smoothing technique

✉ Corresponding author.
E-mail address: 20151536@huanghuai.edu.cn (Y. Ji).
Received 20 July 2024; Revised 10 October 2024; Accepted 05 February 2025; Published Online 16 April 2025.
DOI: 10.61091/jcmcc127b-043

1. Introduction

Wushu is one of the most beautiful treasures of traditional Chinese culture and one of the calling cards of Chinese civilization. It has a high reputation in Western countries, and "Chinese Kung Fu" is almost a household word. Among the many schools of martial arts, there are some common basic movements, which are often referred to as the basic skills of martial arts. The basic movements of wushu contain a wealth of mechanical principles, and if we can focus on the use of mechanical knowledge in practice, it will inevitably have a positive impact on the practice of these basic movements, and promote the improvement of the movement level of wushu enthusiasts and wushu athletes [1-4].

With the continuous development of competitive wushu, coaches and athletes often take the difficult movements in wushu sports as the goal of training. However, the irrationality of training methods has led to the injury of wushu set athletes become a common phenomenon, and the injury site is mostly knee joint, and the injury stage is mostly manifested in the landing stage [5-6]. In today's rapid development of modern science and technology, with the help of advanced instruments to quantitatively analyze the technical movements of wushu, especially the more difficult technical movements, can deepen the understanding of the technical movements of wushu and explore the rules of difficult movements, can find the training skills of the movements and prevent the occurrence of injuries [7-11]. Through the use of modern camera measurement technology, combined with the principle of sports biomechanics to analyze the characteristics of the parameters of each stage, summarized the main factors affecting human injury in each stage of the performance of wushu movements, which can provide a reference basis for coaches and athletes engaged in the project to carry out scientific training [12-15].

The purpose of this study is to establish a finite element model for the mechanical analysis of wushu movements, and to extract the kinematic and kinetic data of the movement process based on the basic wushu steps of squatting horse stance, lunge stance and servant stance, to calculate the internal biomechanical properties of the knee joint using the finite element model, and to analyze the mechanism of its damage to the knee joint cartilage and meniscus. The changes of knee joint angle, ground direction force and center of mass movement were simulated by the model. Further finite element analysis of ankle joint injuries in wushu step-and-turn movements provides an experimental basis for skills and injury prevention in wushu performances.

2. Finite element modeling for injury prevention based on martial arts movement mechanics

2.1. *Subjects and Methods*

2.1.1. Subjects and tools. Fifteen subjects, aged (25.4±3.6) years, weighing (55.5±6.3) kg, and standing (173.5±6.5) cm, were recruited within a sports academy.The subjects were required to be free of lower limb athletic injuries in the last six months, as well as having a good athletic experience and familiarity with the movement patterns of the Wushu Horse Stance. A Vicon 3D infrared motion capture system [16] was used to complete the subjects' raw kinematic data acquisition. In addition, raw 3D mechanics data acquisition was completed using a Kistler. Visual3D was used for raw data filtering and inverse dynamics calculation, and the cutoff frequencies for kinematic data and ground reaction force data were 15 Hz and 35 Hz, respectively.The Marker point names and locations/roles are shown in Table 1.

Table 1. Marker call and position/action

Marker call	Position/action
RASIS/LASIS	Anterior superior spine
RICST/LICST	The left and right iliac spine
RPSIS/LPSIS	The posterior upper spine of the left and right iliac
SARC	Iliac crest
RTROC/LTROC	The large femur rotor
RTH/LTH1-4	Tracking point
RLEP/LLEP	The lateral condyle of the femur
RMEP/LMEP	The medial condyle of the femur
RSK/LSK1-4	Tracking point
RLME/LLME	The tip of the ankle
RMME/LMME	Ankle tip
RHM1/LHM1	The first metatarsal bone
RHM5/LHM5	The fifth metatarsus
RHEE/LHEE	Right and left
RTOE/LTOE	Calculating step Angle

2.1.2. Experimental content. The subjects underwent 10min warm-up exercises before the martial arts horse step experiment, and then jumped with free swing arm (JFA) and restricted swing arm (JRA) respectively, and landed in the "outer eight" (TO) and normal (BL) postures, a total of 4 situations (free swing arm + normal posture landing is called JFBL, free swing arm + "outer eight" attitude landing is called JFTO, restricted swing arm + normal posture landing is called JRBL, restricted swing arm + "outer eight" posture landing is called JRTO). Each subject is required to jump at 80% of their maximum jump distance, and JRA jumps require subjects to keep their hands on their chest during the jump. The interval between each jump test is 120s, and when touching the ground, both feet fall on different force tables are counted as a successful experiment, and 3 successful data collection times are required.

The experimenter affixed Marker dots named RHEE and RTOE at the heel and second fingertip of the right foot of each subject. In addition, the angle of the force platform was determined as the coordinate origin to establish a laboratory coordinate system, and the coordinates of RHEE and RTOE were obtained based on the trajectories of the Marker points obtained from the Vicon Infrared Motion Capture System, and then the stepping angles could be determined based on a simple constant transformation of trigonometric functions.

2.2. Numerical modeling of the knee joint

In this experiment, an inverse 3D reconstruction [17-18] was performed based on the average of the original CT/MRI data of the right knee joints of five volunteers to obtain the knee joint geometric model, and then to construct an accurate 3D finite element model of the knee joint that conforms to the martial arts horse stance. The knee joint geometric model and the subsequent finite element processing flow are shown in Figure 1.

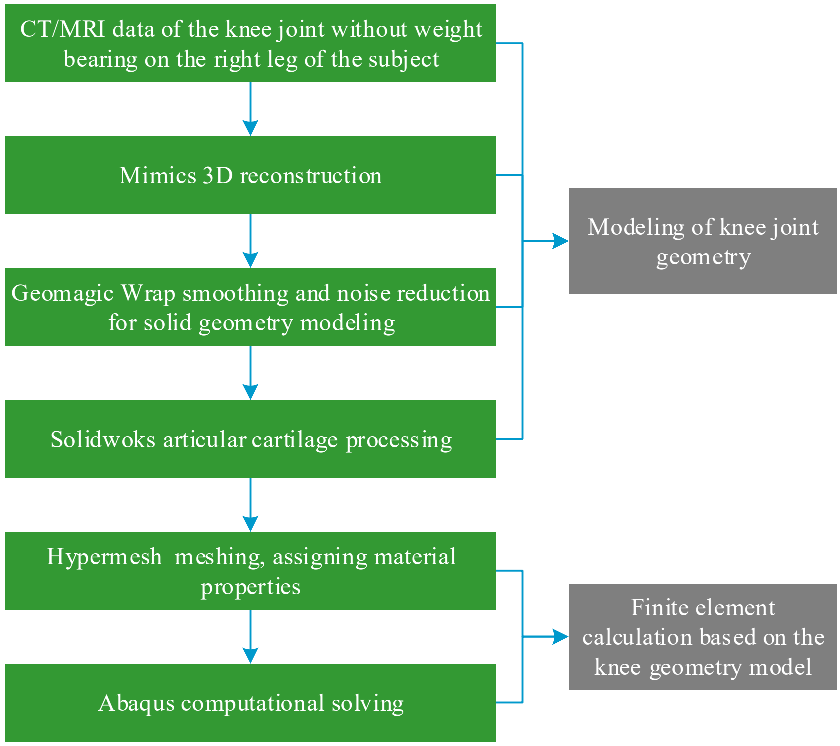

Fig. 1. The joint knee geometry model and the finite element process

2.2.1. Geometric modeling of the knee joint. The combination of CT/MRI scanning was used to accurately reconstruct the femur and tibia in three dimensions, and at the same time to localize the physiological position of the cruciate ligaments, bilateral menisci, femoral cartilage and tibial cartilage plateau.

Subjects were asked to complete the CT/MRI tomography scan in a squatting stance and to remain in a weightless position for half an hour before the scan to avoid stressing the internal tissues and structures of the knee joint.Mimics is a set of highly integrated and easy-to-use 3D image generating and editing software, which can be used to create 3D models based on various scans (CT, MRI), and then output the common CAD (Computer Aided Design), FEA (Computer Aided Design), FEA (Computer Aided Engineering), and FEA (Computer Aided Design) software. Computer Aided Design), FEA (Finite Element Analysis), and RP (Rapid Prototyping) formats. Therefore, the knee tomography data was imported into Mimics 19.0 to complete the 3D reconstruction of the knee joint finite element model.

The bones and soft tissues were separated and masked in Mimics using the CT proprietary grayscale threshold, and the femur, tibia, patella, and fibula were separated using the mask separation function. The 3D inverse reconstruction was performed based on the masks of the separated regions. The reconstructed knee model [19] was imported into Geomagic Wrap for smoothing, geometric feature repair and processing again, and at the same time, the model was transformed into a solid.

Multiple regions of model overlap can occur between closely connected tissues such as bilateral menisci and tibial plateaus. Self-intersections, highly refractive edges, and pinning of the model need to be processed in Wrap, which in turn makes the knee skeletal model more complete and smooth. Importing the Wrap processed knee model into Solidworks for soft tissue processing needs to be combined with the MRI data to be constructed in Solidworks.

2.2.2. Knee joint finite element modeling. Hypermesh software, as the pre-processing software for finite elements, has a more powerful meshing function, so this experiment was calculated by combining Hypermesh finite element pre-processing with Abaqus post-processing. In addition to this, the mesh-independence test (with an error of less than 5%) was performed on the model, and the mesh size of the femur, tibia, fibula and patella was determined to be 2.5 mm, the mesh size of the tibial cartilage plateau was determined to be 2 mm, and the mesh size of the bilateral meniscus and femoral cartilage was determined to be 1 mm. The anterior cruciate ligament (ACL), posterior cruciate ligament (PCL), lateral collateral ligament (LCL), and medial collateral ligament (MCL) within the knee joint were simplified as truss units, which were subjected to tension only and were not compressible. The model material properties and specific parameters are shown in Table 2.

Table 2. Model material properties and specific parameters

Organizational structure	Unit type	Elastic modulus	Poisson ratio	Unit number	Grid size (mm)
Femur	Tetrahedron	12200	0.35	12200	3.5
Patella	Tetrahedron	12200	0.35	20552	3.5
Shin bone	Tetrahedron	12200	0.35	61105	3.5
Fibula	Tetrahedron	12200	0.35	14768	3.5
Femoral cartilage	Hexahedron	18	0.506	18251	2.5
Patella cartilage	Hexahedron	18	0.506	24590	1.5
Tibia cartilage	Hexahedron	18	0.506	1689	1.5
Meniscus	Hexahedron	110	0.513	6150	1.5
MCL	Truss	345	0.513	-	-
ACL\PCL\LCL	Truss	350	0.513	-	-

In addition, ligaments, as the key core for the performance of martial arts squatting horse stance movements, are an important part of maintaining the compliance and stability of the knee joint, mainly including the anterior cruciate ligament (ACL), posterior cruciate ligament (PCL), lateral collateral ligament (LCL), medial collateral ligament (MCL) and other ligaments. The ligaments connect the different tissues of the knee joint, provide ball stability to the joint throughout the range of motion and play an important role in the complex biomechanical changes of the knee joint under different loads. Due to the complexity of the knee joint structure, some finite element studies have represented the mechanical properties of knee ligaments by simplifying the ligaments to one-dimensional truss or sorghum structures and springs.

Four ligaments "ACL, PCL, LCL and MCL" with cross-sections of 40, 55, 20 and 22 mm² were individually modeled using several uniaxial cells with different initial pre-strains. The biggest challenge for 3D ligament finite element modeling is the ability of the material model to distinguish the nonlinear behavior of the ligaments. Therefore, most of the contact analysis studies modeled the ligaments as nonlinear spring elements. And a segmentation function is used to define the behavior of the ligament at low (<5%) and high (>5%) strains.The segmentation function describing the force-displacement relationship of the nonlinear spring element is defined as follows:

$$f = \begin{cases} \frac{1}{4}\kappa\varepsilon^2/\varepsilon & 0 \le \varepsilon \le 2\varepsilon_1 \\ \kappa\left(\varepsilon-\varepsilon_1\right) & \varepsilon > 2\varepsilon_1 \\ 0 & \varepsilon < 0 \end{cases} \tag{1}$$

where f is the ligament tension, k is the spring stiffness parameter, ε_1 is the nonlinear stress parameter, assumed to be 0.05, and ε is the ligament tension, defined as follows:

$$\varepsilon = \left(L - L_0\right)/L_0 \tag{2}$$

where L is the length of the ligament after deformation has occurred, and L_0 is the length of the ligament when it begins to be subjected to tension. L_0 is determined by the initial stress and initial length of the ligament, defined as follows:

$$L_0 = L_r / \left(\varepsilon_r + 1\right) \tag{3}$$

$$\varepsilon_r = \left(L_r - L_0\right) / L_0 \tag{4}$$

where L_r length was determined from MR imaging data and ε_r was obtained from experimental data.

2.3. Wushu Movement Mechanics Data Processing

This study focused on knee biomechanics during the molding phase of martial arts movements, with the impact phase defined as: left lower extremity touchdown to maximum flexion angle of the left knee. Therefore kinematic and kinetic data were intercepted for the landing impact phase. All data were for toe-first touchdown. The moment of touchdown was defined as the moment when the ground reaction force was greater than 15N for 20 consecutive frames.

The kinematics and kinetics were processed in this experiment using Visual 3D software, and the data were smoothed by low-pass filtering using Fourth-order Butterworth. The low-pass filter cutoff frequency was set at 5 Hz for kinematic data and 50 Hz for kinetic data.After the kinematic and kinetic data were processed, the data were time normalized. And the subject's bending angle percentage y, which is the straight line distance from standing to the moment of action shaping x was calculated to normalize the subject's height h with the formula shown below:

$$y(\%) = x / h \tag{5}$$

The kinematic parameter: three-plane angle of the knee joint; and the kinetic parameter: ankle joint reaction force were selected as the boundary conditions and loads for the finite element analysis of the knee joint.

3. Analysis of mechanical damage results of martial arts movements based on the finite element method

3.1. Knee movement angles

In this study, the default in the three planes of knee upright position is zero degree, knee flexion and extension movements are along the X-axis, internal and external rotation along the Y-axis, and internal and external rotation along the Z-axis, and knee extension, adduction and internal rotation are positive angles; knee flexion, abduction and external rotation are negative angles.

This paper explores the three basic step patterns involved in martial arts. The specific stances are described as follows:

Horse stance: legs apart, shoulder-width apart, knees bent, body sinking.

Bow Stance: one foot in front, one foot behind, front leg bent, back leg straight.

Servant Stance: one foot in front, one foot behind, front leg straight, back leg bent, body leaning forward.

3.1.1. Flexion-extension angle of motion of the knee in the x-axis. The X-axis knee joint movement angle is shown in Figure 2. In the horse stance, the knee was in a positive angle, i.e., a certain angle of hyperextension, with a maximum angle of 10°, and the knee was in flexion during the subsequent bracing and propulsion phases, with a maximum flexion angle of -42° at the end of the propulsion phase, when the toes of the foot were off the ergometer. In the lunge, the knee had a maximum flexion angle of -57° at the 80th percentile due to the cushioning effect. In the servant stance, the knee was mostly in a larger flexion angle, and there were two peaks in the curve, the first peak was in the right foot swing phase, and the second peak was produced by the right lower limb extension after the left lower limb landed.

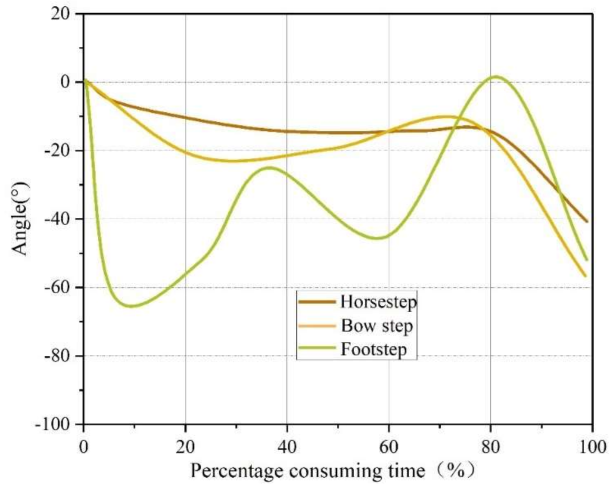

Fig. 2. The Angle of the X-axis knee

3.1.2. Angle of motion of the knee in internal and external rotation on the Y-axis. The Y-axis knee joint movement angle is shown in Figure 3. Horse stance in the process of martial arts movement in the knee joint is mostly in the upright state, the change is small, in about 15 °. In the Y-axis angle curves of the knee joints in the lunge and the servant stance, there are two time periods with large changes in the angle, the first one is about 50% of the time, when the right lower limb starts and completes the outward swinging movement, and the second one is the stomping extension of the right lower limb after the left lower limb touches the ground. The knee joints in the final lunge and servant stance movements showed tilts of about 28° and -11°, respectively.

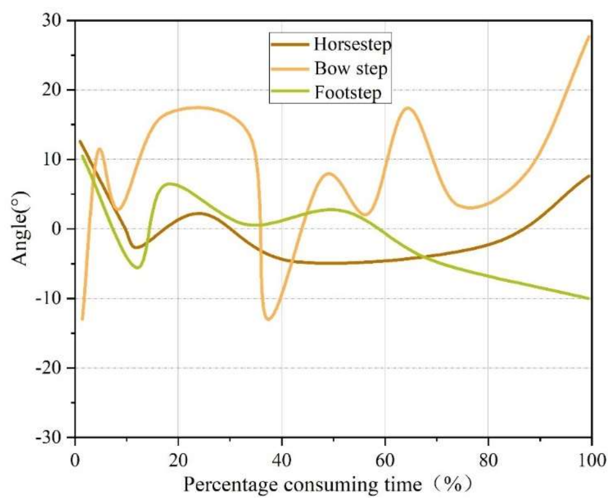

Fig. 3. The Angle of the y axis knee

3.1.3. The angle of motion of the knee in internal and external rotation in the Z-axis. The Z-axis knee joint movement angle is shown in Figure 4. The motion curve of the knee joint on the Z-axis in the squatting horse stance action has a tendency to transition from internal rotation to external rotation, and this process occurs when the time is 10%, at which time the angle of its knee joint bends around -3°; when the time is 90%, the knee anteriorly tilted angle turns from negative to positive, and ultimately becomes positive around 8°. During the lunge and servant step maneuvers, the process appears to have a larger ankle tilt angle because of the extra ankle tilt. The lunge has a knee inclination angle of around -14° at 41% of the time, at a short 68% of the time, the knee tilt angle is around 22°, and at 100% of the time, its knee angle eventually shows -20°. The knee angle of the servant stance went from 13° at the very beginning (at 0% time) to become about 21° at the end (at 100% time), which is believed to be closer to the range of variation than the lunge. The range of knee motion was greater in the lunge and servant stance maneuvers compared to the squat stance.

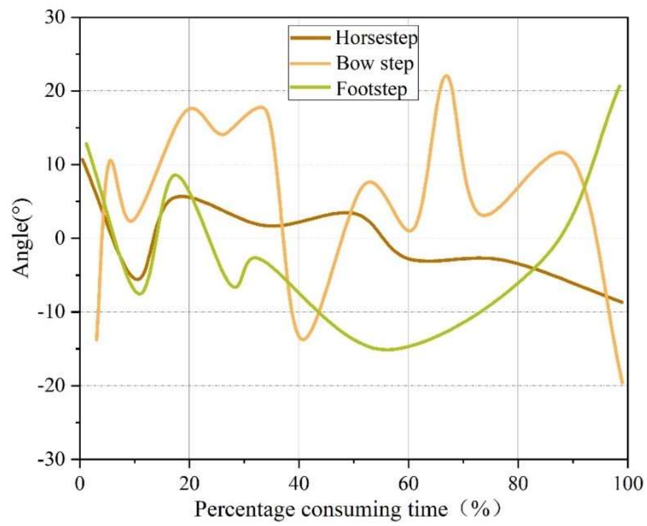

Fig. 4. The Angle of the z axis knee

3.2. Ground reaction forces

The ground reaction force curves for the three maneuvers are shown in Figure 5. The first peak of the ground reaction force of the servant step occurs at the 16% moment, which is generated by cushioning the impact, and has a size of 0.56 times body weight. The second peak occurs at 55% of the time, which is generated by the stomp propulsion, and is 0.92 times the body weight. For the ground reaction force curve of the lunge, the first peak occurs at 15% of the moment, 1.31 times the body weight, and is generated by the cushioning impact. The second peak occurs at 40% of the moment and is 1.7 times the body weight, generated by the propulsive stomp. The ground reaction force curve of the horse stance has no obvious peak characteristics, but there are 2 platform characteristics. The first plateau was during the backward tilt of the center of gravity and was about 1.19 times body weight. The second plateau is the forward leaning state of the center of gravity, with a size of about 1.15 times body weight. There is a “trough” between the first and second plateau phases, which is related to the process of center of gravity backward and forward tilt.

The kinetic data show that the lunge and the horse stance are still characterized by a typical double peak, i.e., the two peak forces generated by landing and reaching. Moreover, the lunge and horse stance have greater peak ground reaction forces than the servant stance. The maximum ground reaction force for the lunge is 1.7 times the body weight, 1.19 times the body weight for the horse stance, and 0.92 times the body weight for the servant stance. It can be found that the ground reaction force curves in wushu movements do not have obvious peak characteristics, and the whole curve is relatively flat.

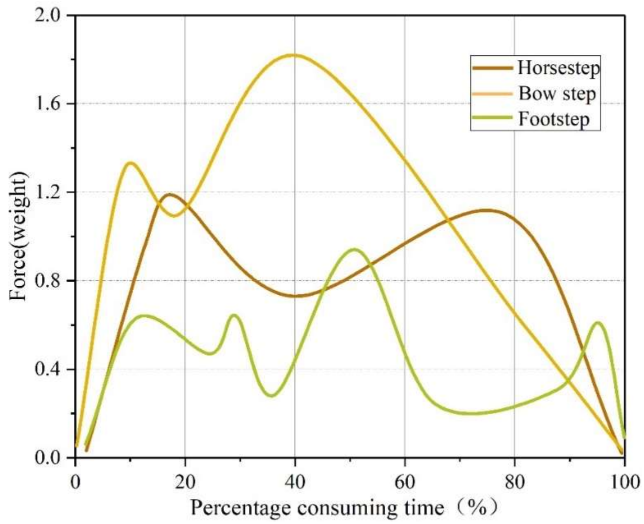

Fig. 5. Three kinds of action surface reaction curve

3.3. *Center of mass shift*

The kinetic rigid body model in this study only modeled the lower limb, so the center of mass calculated here was only the total center of mass of all the links of the lower limb. From the curves, it was found that there was a continuous transition between the horse stance and the lunge from the time the right lower limb stepped into the force platform to the time it left the force platform, and the trend of the lunge and the servant stance was more similar, so only the lunge was chosen as the target movement to complete the center of mass movement test in this paper, and the knee joints of the two movements were twisted to a certain degree in the horizontal plane between the landing cushioning and the stomping and reaching phases, and this feature was more obvious in the straddle-knee arched stance movement, in which the knee joints were twisted to a certain degree. In particular, this feature was more pronounced in the straddle-knee stance. Therefore, in the following analysis, the knee-straddling stance was added.

The center of mass movement in the forward and backward direction is shown in Figure 6; the center of mass movement in the left and right direction is shown in Figure 7; and the center of mass movement in the up and down direction is shown in Figure 8. The center-of-mass movement data show that the horse stance and lunge are continuous in the forward direction with small speed changes, while the knee-straddling stance is in the state of forwarding, adjusting and forwarding again due to the foot swinging outward. In the lunge and horse stance, the center of mass is less shifted to the sides, whereas in the knee-straddle stance, the center of mass is more shifted to the sides due to the external swinging motion. The position of the center of mass is also lower compared to the horse stance and lunge.

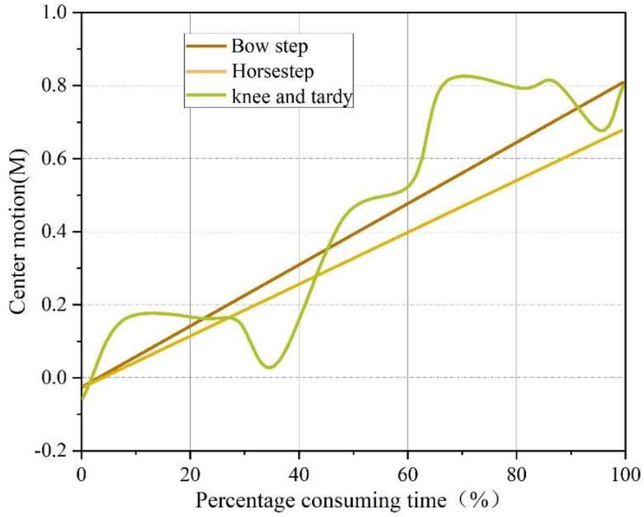

Fig. 6. The result of moving before and after the motion

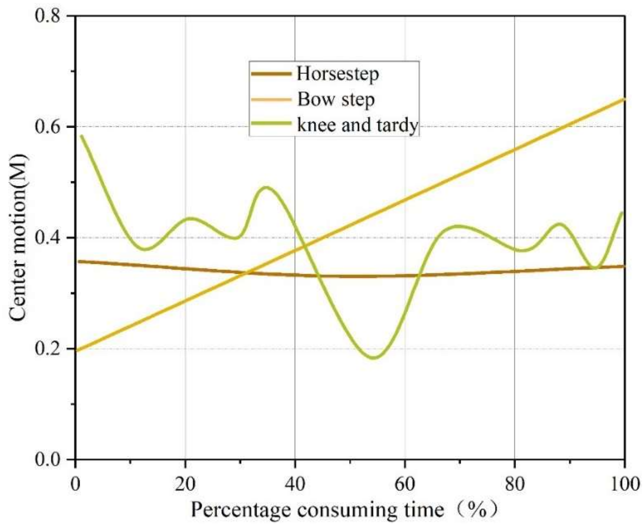

Fig. 7. Movement of the center of motion left and right

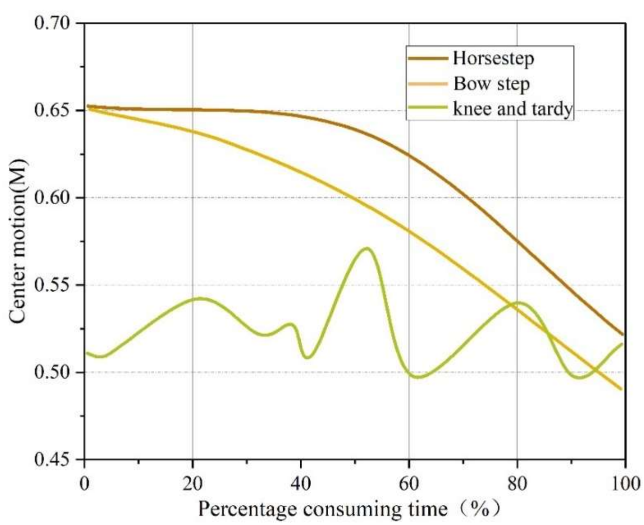

Fig. 8. The result of moving on the motion and below to the center of mass

3.4. Finite element analysis results

In this paper, one kinematic and kinetic data closest to the average value is selected as the loading data for the finite element model of the ankle joint in martial arts movements. The biomechanical data of one tester's straddle-turn maneuver is shown in Figure 9. The results show that there are two peak moments of the ground reaction force in the step-and-turn phase, the dorsiflexion angle of the ankle joint increases after touching the ground and is accompanied by a gradual increase in the external rotation angle and external rotation angle, but the range of change of the external rotation angle is small, and the ankle joint angles of the three axes of motion decrease continuously in the return phase after completing the turning maneuver.

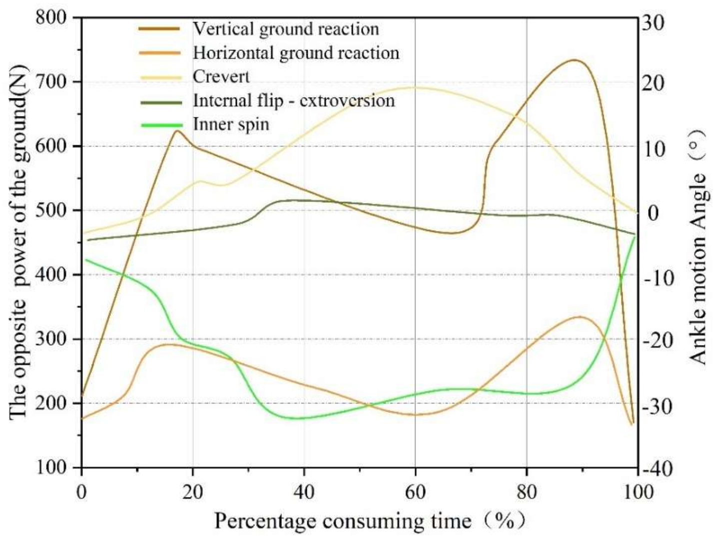

Fig. 9. A test person stepped through the biomechanics data

In this study, a total of 5 characteristic moments were selected for finite element analysis according to the characteristics of the motion changes, but since the maximum external rotation and maximum valgus appeared at the same moment, a total of 4 characteristic moments of kinematic and kinetic data were included in this paper for the biomechanical finite element analysis of the ankle joint in the turn-and-step-turn maneuver.The 4 characteristic moments were as follows (in order of appearance): first ground The four characteristic moments were (in chronological order of appearance): first ground reaction force peak moment (A1), maximum external rotation-external rotation moment (A2), maximum dorsiflexion moment (A3), and second ground reaction force peak moment (A4). The load data from the finite element analysis of the ankle joint for the step-and-turn maneuver are shown in Table 3. The ankle joint angles in the sagittal, coronal, and vertical axes and the values of vertical ground reaction force and horizontal ground reaction force corresponding to the four characteristic moments are: the first peak ground reaction force moment (A1): 5.85°, 1.174°, -11.297°, 605.171N, and 290.027N; the maximal external rotation-external rotation moment (A2): 15.289°, 4.883°, -23.427°, 558.769N, and 224.67N; maximum dorsiflexion moments (A3): 20.295°, 3.772°, -20.334°, 484.871N, and 192.758N; and moments of the peak of the second ground reaction force (A4): 8.13°, 2.846°, - 17.785°, 708.33N, 333.504N.

Table 3. The load data of the finite element analysis of the ankle joint

Characteristic moment	The plantar bending(°)	Internal flip - extroversion(°)	Inner spin(°)	Vertical reaction(N)	Horizontal reaction(N)
The first time of the surface reaction force(A1)	5.85	1.174	-11.297	605.171	290.027
Maximum external rotation - the moment of external turning(A2)	15.289	4.883	-23.427	558.769	224.67
Maximum back bend(A3)	20.295	3.772	-20.334	484.871	192.758
The second surface reaction force peak moment(A4)	8.13	2.846	-17.785	708.33	333.504

Wushu step-and-turn movement is a continuous dynamic movement, but in this study, considering its complexity, accuracy and economy of calculation when performing finite element analysis, biomechanical data of the characteristic moments that may cause higher stress inside the ankle joints as mentioned in previous studies were selected as the load data for calculation and analysis, so as to derive the stress data inside the ankle joints at different characteristic moments and the characteristics of the stress distribution. Situation. Stress is the internal force generated inside the object when the object is deformed by an external force. The results of finite element analysis of stress and stress distribution characteristics are shown in Table 4. The results of finite element analysis show that in the stage of wushu step and turn, the stress distribution of the ankle joint mainly focuses on the tibial tissue, followed by the talus and fibula, and the stress value of the heel bone is relatively small. With the changes of joint angle and ground reaction force, the stress values of the bone tissues inside the ankle joint were also changing, and were positively correlated with the changes of ground reaction force.

In addition, during the step-and-turn phase, the stresses were mainly concentrated in the posterior-lateral tibial subtalar joint surface, the posterior talus, and the proximal fibula, which also made them more vulnerable to injury during the step-and-turn phase. Mechanical loading has both positive and negative effects on the musculoskeletal system. Biologically positive effects include strengthening of the musculoskeletal system due to moderate loading and adequate rest periods, whereas biologically negative effects, e.g., due to overloading, include structural damage to the musculoskeletal system, which may ultimately lead to skeletal muscle damage. Although the concept of a causal relationship between mechanical loading and injury has been established and the relationship between biomechanical variables and overuse injuries has been explored, the exact causes of overuse injuries have not been determined.

Table 4. Finite element analysis stress and stress distribution characteristics result

Characteristic moment	Organizational model	Von mises stress value (MPa)	Stress distribution characteristics
The first time of the surface reaction force(A1)	Shin bone	39.961	The lower part of the lower section is lateral
	Astragal	27.996	After the bone block
	Fibula	7.917	Near end of fibula
	Heel bone	0.304	The posterior medial side of the surface of the joint
Maximum external rotation - the moment of external turning(A2)	Shin bone	37.978	The lower part of the lower section is lateral
	Astragal	28.001	After the bone block
	Fibula	7.019	Near end of fibula
	Heel bone	0.28	The posterior medial side of the surface of the joint
Maximum back bend(A3)	Shin bone	28.027	The lower part of the lower section is lateral
	Astragal	18.996	After the bone block
	Fibula	5.928	Near end of fibula
	Heel bone	0.252	The posterior medial side of the surface of the joint
The second surface reaction force peak moment(A4)	Shin bone	52.112	The lower part of the lower section is lateral
	Astragal	38.01	After the bone block
	Fibula	9.918	Near end of fibula
	Heel bone	0.272	The posterior medial side of the surface of the joint

4. Conclusion

In this paper, the finite element method is used to extract the damage of the knee joint during the performance of wushu movements, and the biomechanical finite element analysis is performed with the kinematic and kinetic data of four characteristic moments.

1) During the horse stance maneuver, the distribution area of the stress peak is also larger relative to the lunge and servant stance due to the larger angle of motion of the knee joint. Compared with the horse stance and lunge, the knee cartilage and meniscus stress peaks generated by the straddling knee arched stance maneuver were smaller.

2) The ground reaction force curves in wushu movements do not have obvious peaks, and the whole curve is relatively flat. However, in contrast, the lunge and horse stance had a larger peak ground reaction force than the servant stance, with maximum ground reaction forces of 1.7, 0.92 and 1.19 times the body weight, respectively.

3) The center of mass movement data showed that the horse stance and lunge movements were continuous in the forward direction, with less change in speed, and the center of mass of both movements moved less to the sides. In contrast, the center of mass of the knee-straddle movement is more varied to both sides, and the center of mass position is lower compared with that of the horse stance and lunge movement.

4) Through the finite element simulation analysis, the peak biomechanical data corresponding to the four characteristic moments of “the first peak ground reaction force moment, the maximum external rotation-external rotation moment, the maximum dorsiflexion moment, and the second peak ground reaction force moment” were obtained in this paper.

Therefore, by wearing protective equipment and monitoring the data during the performance, we can adjust the posture and force generation mode in time to prevent injuries to the injury-prone areas, such as the posterior-lateral tibial subtalar surface, the posterior part of the talus, and the proximal part of the fibula.

References

[1] Yan, S., Chen, J., & Huang, H. (2022). Biomechanical Analysis of Martial Arts Movements Based on Improved PSO Optimized Neural Network. *Mobile Information Systems*, 2022(1), 8189426.

[2] Wang, X., Zhi, C., & Wang, Q. (2017). Research on Wushu Actions and Techniques Based on a Biomechanical Sensor System. *International Journal Bioautomation*, 21(2), 199.

[3] Lei, Z., & Lv, W. (2022). Feature Extraction‐Based Fitness Characteristics and Kinesiology of Wushu Sanda Athletes in University Analysis. *Mathematical Problems in Engineering*, 2022(1), 5286730.

[4] Guo, W. (2018). Application of video feedback system in analysis and diagnosis of Wushu routine movement. *Journal of Interdisciplinary Mathematics*, 21(5), 1187-1191.

[5] Maotang, W., Zhifeng, S., & Mingyong, W. (2023). Joint injuries in martial arts and their preventive measures. *Revista Brasileira de Medicina do Esporte*, 29, e2022_0725.

[6] Xu, M., Jiang, Y., He, X., Yuan, J., & Gao, Y. (2021). Dynamic analysis of the complex motion of three-section cudgel in Wushu sports. *Applied Sciences*, 11(21), 10407.

[7] Cha, J. Y., Lee, H. S., Park, S., & Jee, Y. S. (2021). Effects of Knee Injury Length on Jump Inside Kick Performances of Wushu Player. *Medicina*, 57(11), 1166.

[8] Rashidi, F., Daneshjoo, A., & Sadati, S. K. M. (2020). The effect of corrective feedback exercise on knee kinematics and EMG of lower limbs of female wushu players. *Journal of Modern Rehabilitation*.

[9] Fei Tan, J. (2015). Analysis of the Plantar Pressure Characteristics of Action Flying Kick for Martial Arts Athletes. *The Open Biomedical Engineering Journal*, 9(1).

[10] Gong, M. (2021). Algorithm of Ground Stability Correction for High Difficulty Movements of Competitive. *In Application of Intelligent Systems in Multi-modal Information Analytics: Proceedings of the 2020 International Conference on Multi-model Information Analytics (MMIA2020), Volume 1* (pp. 593-601). Springer International Publishing.

[11] Podrigalo, L. V., Volodchenko, A. A., Rovnaya, O. A., & Stankiewicz, B. (2017). Analysis of martial arts athletes' goniometric indicators. *Physical education of students*, (4), 182-188.

[12] Deliu, R., Stoica, M., & DREVE, A. A. (2021). POSSIBILITIES OF COMPLEX OBJECTIVATION OF TECHNICAL ELEMENTS COMBINATION FROM MARTIAL ARTS WITH THE HELP OF MVN XSENS. *eLearning & Software for Education*, 2.

[13] Levitsky, A. G., Matveev, D. A., & Krutoy, A. N. (2024). Biomechanical analysis of the trajectory of movement of the center of gravity of an athlete in martial arts. *Theory and Practice of Physical Culture*, (2), 27-29.

[14] Irawan, F. A., Nomi, M. T., & Peng, H. T. (2021). Pencak silat side kick in persinas asad: Biomechanics analysis. *International Journal of Human Movement and Sports Sciences*, 9(6), 1230-1235.

[15] Vejar-Robles, J. G., Vega-Gonzalez, A., & Duarte-Zamorano, R. P. (2017). A low-cost methodology for biomechanical analysis of martial arts using videography and accelerometers. *In VII Latin American Congress on Biomedical Engineering CLAIB 2016, Bucaramanga, Santander, Colombia, October 26th-28th, 2016* (pp. 413-416). Springer Singapore.

[16] Rigoni Giulio,Monaco Niccolò,Martinez Garazi Casillas,Cibin Federica,Spolaor Fabiola,Guiotto Annamaria & Sawacha Zimi. (2023). Reliability of an AI driven 3-dimensional markerless motion capture system for on the field sport applications. Gait & Posture(S1),S403-S404.

[17] Zexu Huang,Sarah Monazam Erfani,Siying Lu & Mingming Gong. (2024). Efficient neural implicit representation for 3D human reconstruction. Pattern Recognition110758-110758.

[18] Albert Garifullin,Nikolay Maiorov,Vladimir Frolov & Alexey Voloboy. (2024). Single-View 3D Reconstruction via Differentiable Rendering and Inverse Procedural Modeling†. Symmetry(2),

[19] Chen Jiahe,Yuan Fuzhen,Shen Yu & Wang Junchen. (2021). Multimodality-based knee joint modeling method with bone and cartilage structures for total knee arthroplasty.. The international journal of medical robotics + computer assisted surgery : MRCAS(6),e2316-e2316.